Dyes and Pigments 83 (2009) 148–154

Contents lists available at ScienceDirect

Dyes and Pigments

journal homepage: www.elsevier.com/locate/dyepig

# Characterization of interaction between C.I. Acid Green 1 and human serum albumin: Spectroscopic and molecular modeling method

Yuanyuan Yue, Xingguo Chen*, Jin Qin, Xiaojun Yao

*Department of Chemistry, Lanzhou University, Lanzhou 730000, PR China*

ARTICLE INFO

*Article history:*
Received 9 August 2008
Received in revised form
7 February 2009
Accepted 16 February 2009
Available online 4 March 2009

*Keywords:*
C.I. Acid Green 1
Human serum albumin (HSA)
Resonance light scattering (RLS)
Circular dichroism (CD)
Fourier transformation infrared spectra (FT-IR)
Molecular modeling

ABSTRACT

The binding characteristics of human serum albumin with C.I. Acid Green 1 were studied by employing fluorescence, resonance light scattering, ultraviolet–visible, circular dichroism, Fourier transform infrared techniques and molecular modeling. Spectroscopic analysis has revealed that quenching of human serum albumin by C.I. Acid Green operates by a static quenching mechanism. The results by Fourier transform infrared, circular dichroism and ultraviolet–visible absorption spectra experiment indicated that the secondary structures of protein were changed in the presence of C.I. Acid Green 1. Molecular modeling revealed that a dye–protein complex was stabilized by hydrophobic forces, Van-der-Waals force and hydrogen bonding, via amino acid residues. Furthermore, influences of coexisting substances on the binding constant of C.I. Acid Green 1-human serum albumin complexes were investigated.



## 1. Introduction

C.I. Acid Green 1 (Fig. 1) is an anionic dye. It has been widely used as a biological stain and diagnostic aid. On the other hand, C.I. Acid Green 1 has excellent redox characteristics, thus it can be used as a mediator for electrocatalysis of biological compounds [1,2]. It was reported that some dyes would stain certain tissues, the dyes would selectively stain, combine with and destroy pathogenic organisms without causing appreciable harm to the host [3]. Nowadays, much research on the binding of drugs to HSA has been carried out [4–10], but seldom report on the binding interaction of proteins with the dye. To have a full understanding of the modes of dye–protein interaction is important for understanding the biological effects and functions of dyes in the body.

Human serum albumin (HSA) is the major soluble protein with a high concentration in blood plasma (40 kg/m$^3$ or $0.6 \times 10^{-3}$ mol/L). The structure of HSA has been established and it consists of three structurally homologous, predominantly helical domains (domains I, II and III), with each domain containing of two subdomains (A and B). X-ray measurements have revealed that ligands binding to HSA are located in hydrophobic cavities in subdomains IIA and IIIA referred to as Sudlow sites I and II [11,12]. Except from maintaining colloid osmotic pressure, HSA also plays a role in transport of a number of ligands including hormones, hemin, bilirubin and fatty acids, as well as transition metals such as copper, cobalt, nickel, and cadmium [13,14]. Dye-protein interaction can affect the duration and intensity of pharmacological effect [15]. Investigation on the interaction of HSA with a dye can help us better understand the absorption and distribution of dye, and hence become an important research field in chemistry, life sciences and clinical medicine.

The interaction of HSA with C.I. Acid Green 1 was demonstrated via fluorescence spectroscopy, ultraviolet–visible (UV–vis), resonance light scattering (RLS), Fourier transformed infrared (FT-IR), and circular dichroism (CD) approaches. The binding constants were obtained at different temperatures in the medium of HCl–Tris (pH 7.40) buffer solution. Information regarding the binding sites and main types of binding force of the reaction was provided. The conformational changes of HSA were discussed on the basis of synchronous fluorescence spectra, CD and FT-IR. In addition, the partial binding parameters of the reaction were calculated through SGI FUEL work stations.

## 2. Materials and methods

### 2.1. Materials

Human serum albumin (fatty acid free $< 0.05\%$) was purchased from Sigma Chemical Co. and used without further purification.

* Corresponding author. Tel.: +86 931 8912763; fax: +86 931 8912582.
*E-mail address:* chenxg@lzu.edu.cn (X. Chen).

0143-7208/$ – see front matter © 2009 Elsevier Ltd. All rights reserved.
doi:10.1016/j.dyepig.2009.02.010

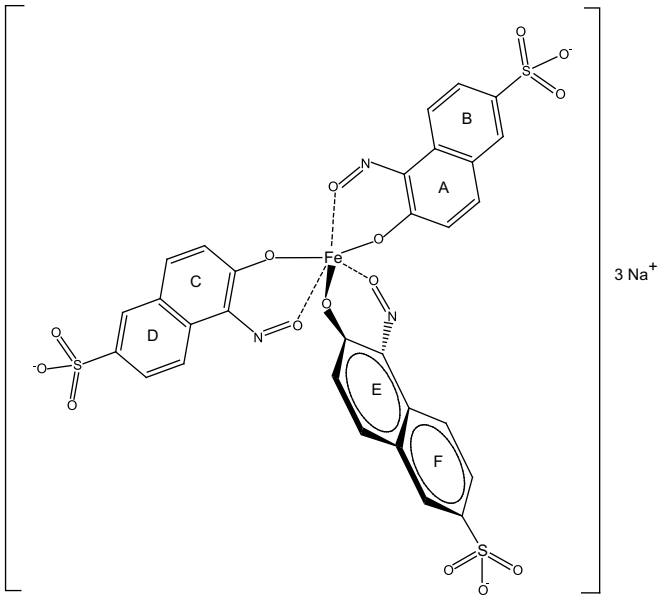


**Fig. 1.** Chemical structure of C.I. Acid Green 1.

C.I. Acid Green 1 (analytical grade) was obtained from Xi-an huaxue shijichang (China), and the stock solution was prepared in water. All HSA solution was prepared in the pH 7.40 buffer solution, and HSA stock solution was kept in the dark at 4 °C. Buffer (pH 7.40) consists of Tris (0.2 mol/L) and HCl (0.1 mol/L), and the pH was adjusted to 7.40 by 0.5 mol/L NaOH when the experiment temperature was higher than 296 K. The pH was checked with a suitably standardized pH meter. All reagents were of analytical reagent grade and double distilled water was used throughout the experiment.

### 2.2. Spectroscopic measurements

Fluorescence measurement and the spectrum of resonance light scattering (RLS) were obtained with an RF-5301PC spetrofluorophotometer (Shimadzu). The fluorescence emission spectra were recorded from 290 to 500 nm (excitation wavelength 280 nm) using 5/5 nm slit widths. Synchronous fluorescence spectra of HSA in the absence and presence of increasing amount of C.I. Acid Green 1 were recorded. UV–vis absorption measurements were performed on Shimadzu UV-240 spectrophotometer with a 1.0 cm quartz cell at room temperature. An electronic thermoregulating water bath (NTT-2100, EYELA, Japan) was used to control the temperature of the samples.

FT-IR measurements were carried out at a constant room temperature (296 K) on a Nicolet Nexus 670 FT-IR spectrometer (America) equipped with a germanium attenuated total reflection (ATR) accessory, a DTGS KBr detector and a KBr beam splitter. All spectra were taken via the attenuated total reflection (ATR) method with resolution of 4 $cm^{-1}$ and 60 scans. Spectra of buffer solution were collected at the same condition, then, the absorbance of buffer solution was subtracted from the spectra of sample solution to get the FT-IR difference spectra of proteins. The subtraction criterion was that the original spectrum of protein solution between 2200 and 1800 $cm^{-1}$ was featureless [16].

The CD spectra were gained by Olis DSM1000CD (USA) with a 0.1 cm quartz cell at room temperature, the speed of scanning was 30 nm $min^{-1}$, the slit width was set at 5 nm. The induced ellipticity was obtained by the ellipticity of the dye–HSA mixture subtracting the ellipticity of dye at the same wavelength and is expressed in degrees. The results were expressed as mean residue ellipticity (MRE) in deg $cm^2$/dmol, which is defined as [MRE $\theta_{obs}$ (mdeg)/$10nlC_p$]. The $\theta_{obs}$ represents the CD in millidegree, $n$ is the number of amino acid residues (585), $l$ the path length of the cell and $C_p$ is the mole fraction [17]. The α-helical content of HSA was calculated from the MRE value at 208 nm using (Eq. (1)) as described by Khan et al [18].

$$\alpha - helical\% = [(MRE\ 208 - 4000)/33,000 - 4000] \times 100 \quad (1)$$

### 2.3. Molecule modeling

A docking study of the binding mode between drug and HSA was performed on SGI Fuel workstation. The crystal structure of HSA in complex with *R*-warfarin was downloaded from the Brookhaven Protein Data Bank (entry codes 1h9z) [19]. The potential of the 3-D structures of HSA was assigned according to the Amber 4.0 force field with Kollman-all-atom charges. The initial structures of all the molecules were generated by molecular modeling software Sybyl 6.9 [20]. The geometry of the molecule was subsequently optimized to minimal energy using the Tripos force field with Gasteiger–Marsili charges with a gradient of 0.005 kcal/mol. FlexX program was applied to calculate the interaction mode between dye and HSA. During the docking process, a maximum of 30 conformers was considered for this compound. The conformer with the lowest binding free energy was used for further analysis.

## 3. Result and discussion

### 3.1. The binding mechanism analysis of C.I. Acid Green 1 and HSA

Fluorescence quenching is the decrease of quantum yield of fluorescence from a fluorophore induced by a variety of molecular interactions with a quencher molecule. The application of fluorescence measurements can reveal the reactivity of chemical and biological systems since it allows non-intrusive measurements of substances in low concentration under physiological conditions. Fig. 2 shows the fluorescence spectrum of HSA in pH = 7.40 buffer solution at $\lambda_{ex} = 280$ nm. Addition of different concentrations of C.I. Acid Green 1 caused a noticeable decrease in HSA fluorescence intensity, and an increase in the fluorescence intensity at 450 nm was assigned to C.I. Acid Green 1. Moreover, the occurrence of an isobestic point at 410 nm might also indicate the existence of bound

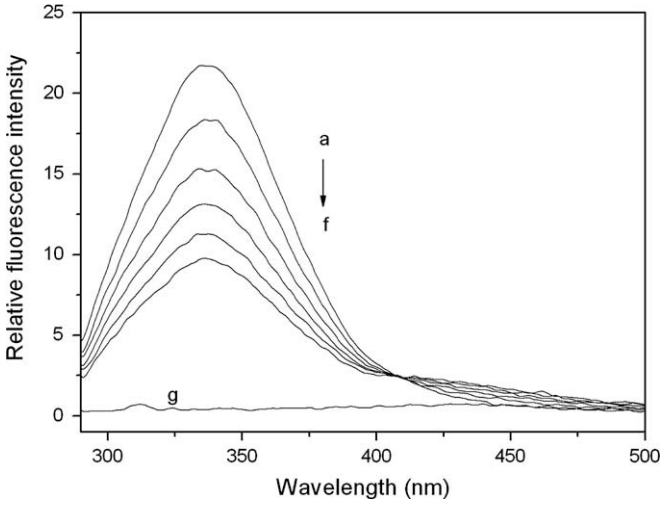


**Fig. 2.** Fluorescence spectra of C.I. Acid Green 1–HSA system ($T = 298$ K, pH 7.40). (a) $3.0 \times 10^{-6}$ mol/L HSA; (b)–(f) $3.0 \times 10^{-6}$ mol/L HSA in the presence of 3.32, 6.62, 9.90, 13.16, 16.39 $\times 10^{-6}$ mol/L C.I. Acid Green 1; (g) $3.32 \times 10^{-6}$ mol/L C.I. Acid Green 1.

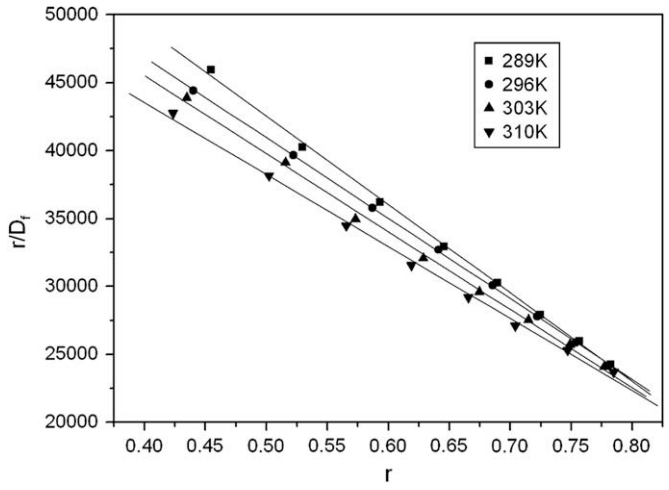


**Fig. 3.** The Scatchard curves for the binding of C.I. Acid Green 1 to HSA at pH 7.40. [HSA] = $3.0 \times 10^{-6}$ mol/L; $\lambda_{ex} = 280$ nm, and $\lambda_{em} = 339$ nm.

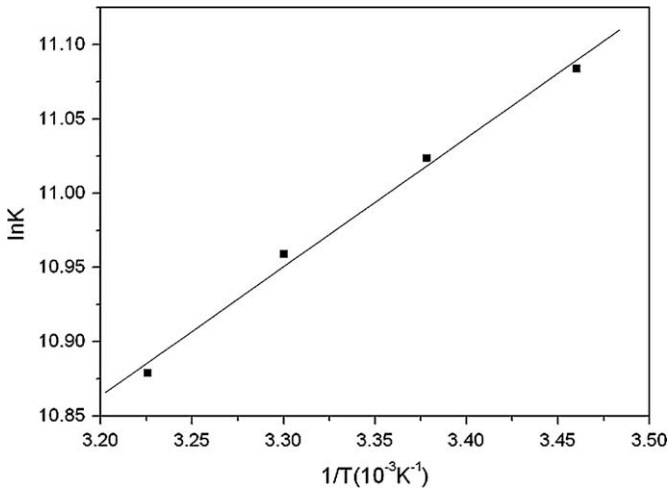


**Fig. 4.** Van't Hoff plot for the interaction of HSA and C.I. Acid Green 1 in Tris buffer, pH 7.40.

and free C.I. Acid Green 1 in equilibrium. These results indicated that there was a strong interaction and energy transfer between C.I. Acid Green 1 and HSA [21].

The possible quenching mechanism can be deduced from the Scatchard equation [22].

$$r/D_f = nK - rK \tag{2}$$

where $r$ represents the number of moles of bound drug per mole of protein, $D_f$ represents the molar concentration of free dye, $n$ and $K$ are the number of binding sites and binding constant, respectively. The Scatchard plot for C.I. Acid Green 1–HSA system at different temperatures is shown in Fig. 3. The satisfactory linearity of Scatchard plots indicated that C.I. Acid Green 1 bound to a class of binding sites on HSA with the increase of the temperature, and the slopes decreased with increasing temperature, which was consistent with the static type of quenching mechanism. The binding constants at different temperatures are shown in Table 1. It was shown that the binding between C.I. Acid Green 1 and HSA was remarkable and the effect of temperature was small.

### 3.2. Binding mode

The acting forces between molecular and a macromolecule mainly include hydrogen bonding, van-der-Waals force, electrostatic force, hydrophobic interaction force, etc. The thermodynamic parameters, enthalpy ($\Delta H^0$) and entropy ($\Delta S^0$) of reaction are important for confirming binding mode. In order to gain the binding mode of the interaction, the temperature-dependence of the binding constant was studied. The temperatures chosen were 289, 296, 303 and 310 K at which HSA did not undergo any structural degradation. If the $\Delta H^0$ does not vary significantly over the temperature range studied, its value and that of $\Delta S^0$ can be evaluated from the Van't Hoff equation:

$$\ln K_T = -\Delta H^0/RT + \Delta S^0/R \tag{3}$$

$$\Delta G^0 = \Delta H^0 - T\Delta S^0 \tag{4}$$

where $K_T$ is the binding constant at the corresponding temperature, $R$ is the gas constant, $T$ is absolute temperature. The values of $\Delta H^0$ and $\Delta S^0$ were obtained from linear Van't Hoff plot (Fig. 4). The $\Delta G^0$ is estimated from Eq. (4). The values of $K$, $\Delta H^0$, $\Delta S^0$ and $\Delta G^0$ are summarized in Table 1. Ross and Subramanian [23] have characterized the sign and magnitude of the thermodynamic parameter associated with various individual kinds of interaction that may take place in protein association processes. The negative sign for $\Delta G^0$ means that the binding process was spontaneous and for typical hydrophobic interactions, both $\Delta H^0$ and $\Delta S^0$ are positive, while negative $\Delta H^0$ and $\Delta S^0$ changes arise from van-der-Waals force and hydrogen bonding formation in low dielectric media. Therefore, it is more likely that hydrophobic interaction was involved in its binding process.

**Table 1**
Binding parameters and thermodynamic parameters of C.I. Acid Green 1–HSA.

| pH | $T$ (K) | $K$ ($\times 10^4$ mol$^{-1}$) | $n$ | $\Delta G^0$ (kJ mol$^{-1}$) | $\Delta S^0$ (J mol$^{-1}$ K$^{-1}$) | $\Delta H^0$ (kJ mol$^{-1}$) |
|---|---|---|---|---|---|---|
| 7.40 | 289 | 6.51 | 1.15 | −26.64 | 67.22 | −7.22 |
| | 296 | 5.93 | 1.19 | −27.11 | | |
| | 303 | 5.75 | 1.19 | −27.59 | | |
| | 310 | 5.30 | 1.22 | −28.06 | | |

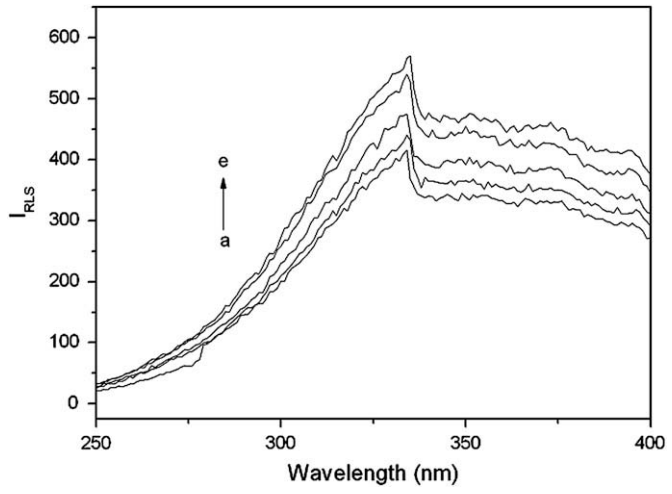


**Fig. 5.** RLS spectra of C.I. Acid Green 1–HSA: (a) $3.0 \times 10^{-6}$ mol/L C.I. Acid Green 1; (b)–(e) $3.0 \times 10^{-6}$ mol/L C.I. Acid Green 1 in the presence of 3.32, 6.62, 9.90, $13.16 \times 10^{-6}$ mol/L HSA.

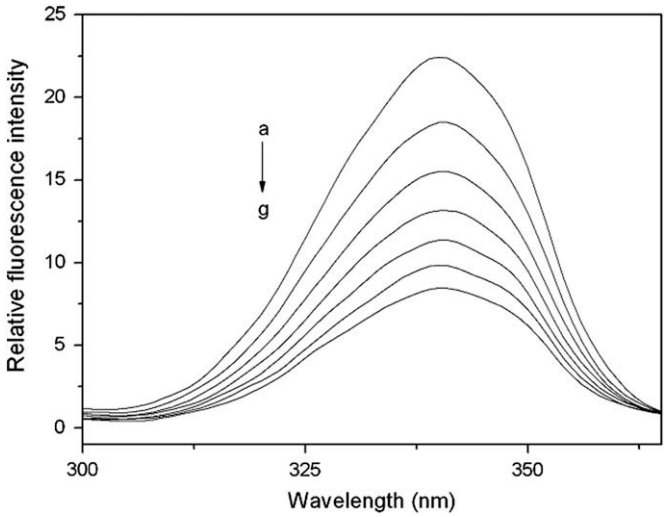


**Fig. 6.** Synchronous fluorescence spectra of interaction between HSA and C.I. Acid Green 1 at $\Delta\lambda = 60$ nm: (a) $3.0 \times 10^{-6}$ mol/L HSA; (b)–(g) $3.0 \times 10^{-6}$ mol/L HSA in the presence of 3.32, 6.62, 9.90, 13.16, 16.39, 19.61 $\times 10^{-6}$ mol/L C.I. Acid Green 1.

### 3.3. RLS spectra

RLS spectra of C.I. Acid Green 1–HSA complex and C.I. Acid Green 1 under optimum conditions are shown in Fig. 5. It can be observed that the intensity of RLS changed appreciably when HSA was added to C.I. Acid Green 1, which indicates that C.I. Acid Green 1 reacted with HSA and formed the C.I. Acid Green 1–HSA complex.

### 3.4. SF, UV–vis, FT-IR and CD spectra

The synchronous scanning technique maintains a constant-wavelength difference ($\Delta\lambda$) between emission and excitation wavelengths. According to Miller [24], distinction of the difference between excitation wavelength and emission wavelength ($\Delta\lambda = \lambda_{em} - \lambda_{ex}$) reflects the spectra of a different nature of chromophores, with large $\Delta\lambda$ values such as 60 nm, the synchronous fluorescence of HSA is characteristic of tryptophan residues. Fig. 6 illustrates SF spectra of HSA adding various amounts of C.I. Acid Green 1 at pH 7.40. It can be observed that there was a slight blue-shift at pH 7.40. The slight blue-shift indicated that the interaction of C.I. Acid Green 1 with HSA may cause conformational change of HSA.

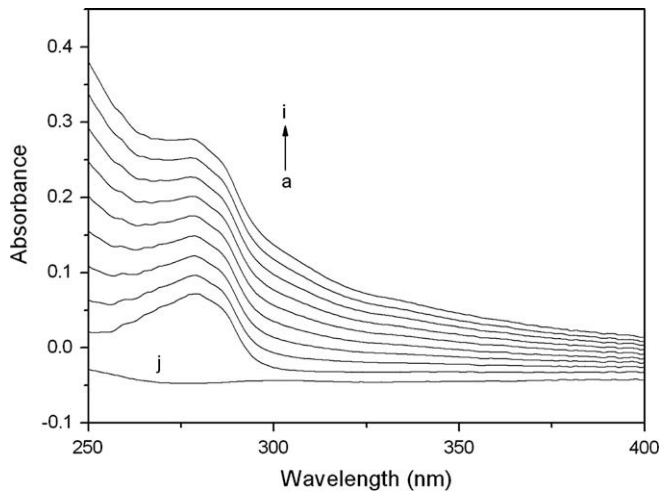


**Fig. 7.** UV absorption spectra of HSA in the absence and presence of C.I. Acid Green 1. C.I. Acid Green 1 concentrations: (a–i) 0, 3.32, 6.62, 9.90, 13.16, 16.39, 19.61, 22.80, 25.97 $\times 10^{-6}$ mol/L; [HSA] = $3.0 \times 10^{-6}$ mol/L; (j) the spectra of V, pH = 7.40, $T = 298$ K.

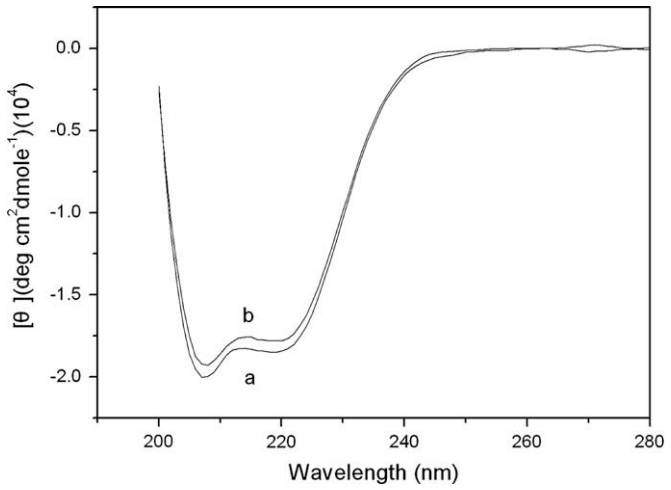


**Fig. 8.** CD spectra of C.I. Acid Green 1–HSA complexes at pH 7.40; $T = 298$ K: (a) $3.0 \times 10^{-6}$ mol/L HSA; (b) $3.0 \times 10^{-6}$ mol/L HSA + $6.0 \times 10^{-6}$ mol/L C.I. Acid Green 1.

UV–vis absorption measurement is a very simple method to explore the structural change of HSA. Fig. 7 is the UV–vis absorption spectra of C.I. Acid Green 1, HSA, and C.I. Acid Green 1–HSA system. As can be seen in Fig. 7, the UV absorption intensity of HSA was increased with the addition of C.I. Acid Green 1, which indicated that it was due to complex formation between C.I. Acid Green 1 and HSA [25] and changed HSA conformation.

In order to obtain more information on C.I. Acid Green 1–HSA interactions, CD measurements were performed on HSA and C.I. Acid Green 1–HSA systems. The CD spectra of HSA exhibit two negative bands at 208 and 222 nm, which are characteristic of an α-helix in the advanced structure of protein. The changes in the spectra at these wavelengths may be used to examine shifts in a-helical content of the protein. The reasonable explanation is that the negative peaks between 208–209 and 222–223 nm are both contributed by n → π* transfer for the peptide bond of α-helical [26].

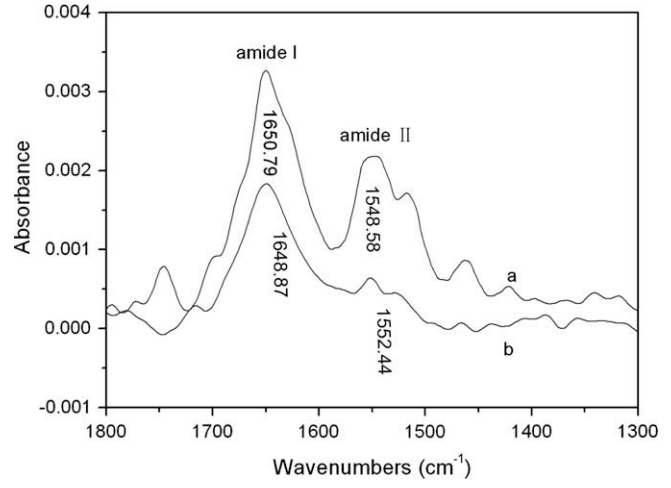


**Fig. 9.** FT-IR spectra of free HSA (a) and different spectra [(HSA solution + C.I. Acid Green 1 solution) – (C.I. Acid Green 1 solution)] (b) in buffer solution in the region of 1800–1300 $cm^{-1}$, [HSA] = $3.0 \times 10^{-5}$ mol/L, [C.I. Acid Green 1] = $6.0 \times 10^{-5}$ mol/L, pH = 7.40, $T = 298$ K.

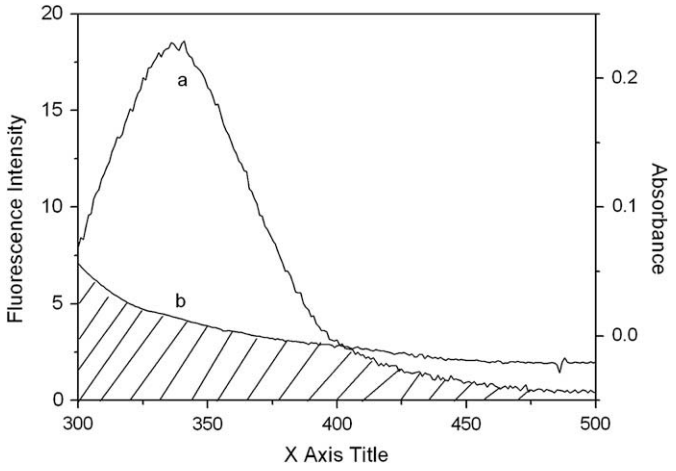


**Fig. 10.** Spectral overlap of HSA fluorescence (a) with C.I. Acid Green 1 (b) $C_{dye}/C_{HSA} = 1{:}1$. pH = 7.40, $T = 298$ K.

Fig. 8 shows that the CD spectra of free HSA have a characteristic of the typical ($\alpha + \beta$)-helix structure with negative bands at 208 and 219 nm. The binding of C.I. Acid Green 1 to HSA decreased both of these bands, indicating the considerable changes in the protein secondary structure with the reduction of the $\alpha$-helical content in HSA and the increase of the disorder structure content in the protein, and it may be the result of the formation of complex between C.I. Acid Green 1 and HSA. The $\alpha$-helical content of HSA was calculated from Eq. (1). The calculated results exhibited a reduction of $\alpha$-helical structures from 55.24 to 52.80 at a molar ratio of HSA to C.I. Acid Green 1 of 1:2.

Further evidence of dye–protein complexation comes from IR spectroscopic results. Infrared spectra of proteins exhibit a number of the amide bands, which represent different vibrations of the peptide moiety. Among these amide bands of the protein, amide I peak position occur in the range in the region 1600–1700 $cm^{-1}$ (mainly C═O stretch) and amide II band in the region 1500–1600 $cm^{-1}$ (C–N stretch coupled with N–H bending mode). As shown in Fig. 9, the peak position of amide I of HSA moved from 1650.79 to 1648.87 $cm^{-1}$ after addition of C.I. Acid Green 1. The result indicated that C.I. Acid Green 1 interacted with the C═O and C–N groups in the protein polypeptides. Because the C.I. Acid Green 1–HSA complexes caused the rearrangement of the polypeptide carbonyl hydrogen bonding network, the protein $\alpha$-helical structure was reduced.

### 3.5. Energy transfer between HSA and C.I. Acid Green 1

Forster non-radiative energy transfer theory (FRET) [27] was used to determine the distances between the protein residue (donor) and the bound dye (acceptor) in HSA. The energy transfer efficiency ($E$) is defined by Eq. (5):

$$E = 1 - F/F_0 = R_0^6 \Big/ \left(R_0^6 + r^6\right) \tag{5}$$

where $r$ is the binding distance between donor and receptor, and $R_0$ is the critical distance when the efficiency of transfer is 50%.

$$R_0^6 = 8.79 \times 10^{-25} k^2 N^{-4} \Phi J \tag{6}$$

$$J = \left(\sum F(\lambda)\varepsilon(\lambda)\lambda^4 \Delta\lambda\right) \Big/ \left(\sum F(\lambda)\Delta\lambda\right) \tag{7}$$

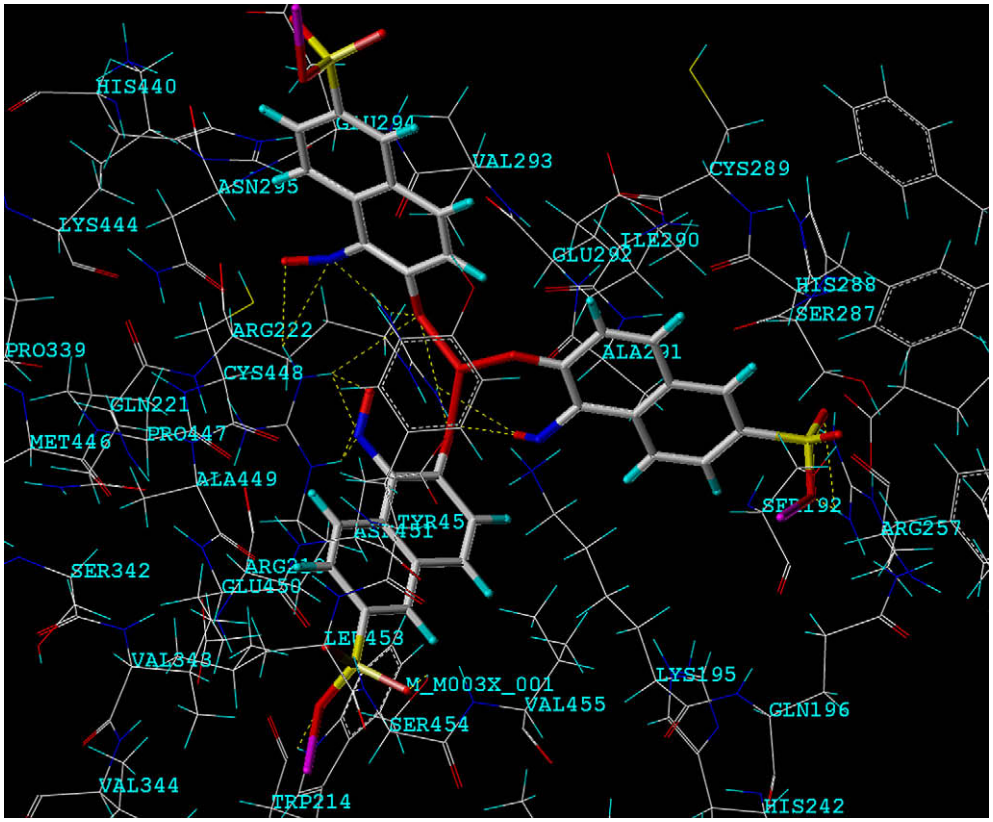


**Fig. 11.** The interaction mode between C.I. Acid Green 1 and HSA (only residues around 6.5 Å of the ligand are displayed). The residues of HSA are represented using line and the ligand structure is represented using ball and stick model. The hydrogen bond between C.I. Acid Green 1 and HSA is represented using a dashed line.

**Table 2**
Effects of coexisting substances ($6.67 \times 10^{-6}$ mol/L) on HSA–C.I. Acid Green 1 system.

| System | Binding constant ($mol^{-1} \times 10^4$) |
|---|---|
| HSA + C.I. Acid Green 1 | $5.87 \pm 0.030$ |
| HSA + C.I. Acid Green 1 + $Zn^{2+}$ | $5.57 \pm 0.041$ |
| HSA + C.I. Acid Green 1 + $Ni^{2+}$ | $5.48 \pm 0.014$ |
| HSA + C.I. Acid Green 1 + $Fe^{3+}$ | $5.59 \pm 0.025$ |
| HSA + C.I. Acid Green 1 + $Al^{3+}$ | $4.19 \pm 0.036$ |
| HSA + C.I. Acid Green 1 + $Cu^{2+}$ | $4.78 \pm 0.008$ |
| HSA + C.I. Acid Green 1 + $Mn^{2+}$ | $4.84 \pm 0.032$ |
| HSA + C.I. Acid Green 1 + L-Leu–OH | $3.83 \pm 0.027$ |
| HSA + C.I. Acid Green 1 + L-proline | $4.63 \pm 0.045$ |
| HSA + C.I. Acid Green 1 + L-lysin | $3.62 \pm 0.029$ |
| HSA + C.I. Acid Green 1 + L-isoleucine | $4.48 \pm 0.018$ |

In Eq. (6), $K^2$ is the spatial orientation factor of the dipole, $N$ is the refractive index of the medium, $\Phi$ is the fluorescence quantum yield of the donor, and $J$ is the overlap integral of the fluorescence emission spectrum of the donor with the absorption spectrum of the acceptor (Fig. 10), which can be calculated by Eq. (7). Where $F(\lambda)$ is the fluorescence intensity of the fluorescent donor at wavelength $\lambda$; and $\varepsilon(\lambda)$ is the molar absorption coefficient of the acceptor at wavelength $\lambda$. In the present case, $K^2 = 2/3$, $N = 1.336$, $\Phi = 0.118$ [28]. According to Eqs. (5)–(7), we could calculate that $R_0 = 1.49$ nm; $E = 0.32$ and $r = 1.69$ nm. Obviously, they are lower than 7 nm after interaction between C.I. Acid Green 1 and HSA. These data suggested that the energy transfer from HSA to C.I. Acid Green 1 occurred with high probability.

### 3.6. Molecular modeling study

Protein-ligand molecular modeling was performed to identify the primary binding site that C.I. Acid Green 1 was located in. Descriptions of the 3-D structure of crystalline albumin showed that HSA is made up of three homologous domains (I, II, and III): I (residues 1–195), II (196–383), and III (384–585); each domain has two subdomains (A and B). The principal regions of ligand binding to HSA are located in hydrophobic cavities in subdomains IIA and IIIA, which are consistent with sites I and II, respectively, and one tryptophan residue (Trp-214) of HSA is in subdomain IIA. The best energy ranked results are shown in Fig. 11. It was important to note that the tryptophan residue (Trp-214) of HSA are in close proximity to the dye molecule suggesting the existence of hydrophobic and Van-der-Waals interactions between them. Further, this finding provided a good structural basis to explain the very efficient fluorescence quenching of HSA emission in the presence of C.I. Acid Green 1. There were also hydrogen interactions between the A-ring of dye and the residue Lys195, C-ring and Arg222, E-ring and Ser454, F-ring and Trp-214 from the IIA subdomain. The calculated binding Gibbs free energy ($\Delta G^0$) was $-27.11$ kJ mol$^{-1}$, which was close to the experimental data ($-28.08$ kJ mol$^{-1}$) to some degree. The results obtained from modeling suggested that C.I. Acid Green 1 could interact with HSA at site I in subdomain IIA, and the interaction between C.I. Acid Green 1 and HSA was dominated by hydrophobic force, Van-der-Waals force and hydrogen bonding.

### 3.7. Influences of coexisting substances on binding constant

The influence of coexisting substances, such as metal ions and amino acids was studied. As shown in Table 2, the binding constants between the C.I. Acid Green 1 and HSA decreased in various degrees in the presence of metal ions and amino acids. This is likely caused by a conformational change in the vicinity of the binding site. There is no direct competition between C.I. Acid Green 1 and metal ions or amino acids, because of different domain they located. Consider its pharmacokinetics, the increase of the binding constant will likely buffer the dye in the blood in some degree [29]. The main reason for the decreased constant may be enhance the toxic effects and decrease the activity of HSA [30].

## 4. Conclusions

In this paper, the interaction between HSA and C.I. Acid Green 1 has been studied by fluorescence, resonance light scattering, UV–vis, circular dichroism, FT-IR techniques and molecular modeling. From the thermodynamic parameter calculation, it showed that the acting force was mainly the hydrophobic. The distance ($r$) between donor and acceptor was obtained according to Forster non-radioactive resonance energy transfer theory. In addition, the results of UV–vis, CD, FT-IR, and synchronous fluorescence spectra indicated that the secondary structure of the protein was changed in the presence of C.I. Acid Green 1. The binding constants of C.I. Acid Green 1–HSA were decreased in the presence of coexisting substances.

## References


[1] Zhao Q, Yuan R, Mo CL, Chai YQ, Zhong X. A new amperometric glucose with Naphthol Green B as mediator. Chinese Chemical Letters 2004;2:208–11.
[2] Cai X, Xue KH. Electrochemical characterization of electropolymerized film of Naphthol Green B and its electrocatalytic activity toward NADH oxidation. Microchemical Journal 1998;58:197–208.
[3] Shaikh SMT, Seetharamappa J, Ashoka S, Kandagal PB. A study of the interaction between bromopyrogallol red and bovine serum albumin by spectroscopic methods. Dyes and Pigments 2007;73:211–6.
[4] He HM, Cater DC. Atomic structure and chemistry of human serum albumin. Nature 1992;358:209–15.
[5] Petitpas I, Crune T, Battacharya AA, Curry ST. Crystal structures of human serum albumin complexed with monounsaturated and polyunsaturated fatty acids. Journal of Molecular Biology 2001;314:955–60.
[6] Trynda-Lemiesz L, Karacyzn A, Keppler BK, Kozlowski H. Studies on the interactions between human serum albumin and trans-indazolium (bisindazole) tetrachlororuthenate(III). Journal of Inorganic Biochemistry 2000;78:341–6.
[7] Pelton JT, Mclean LR. Spectroscopic methods for analysis of protein secondary structure. Analytical Biochemistry 2000;277:167–76.
[8] Jiang M, Xie MX, Zheng D, Liu Y, Li XY, Chen X. Spectroscopic studies on the interaction of cinnamic acid and its hydroxyl derivatives with human serum albumin. Journal of Molecular Structure 2004;692:71–80.
[9] Trynda-Lemiesz L. Paclitaxel–HSA interaction. Binding sites on HSA molecule. Bioorganic & Medicinal Chemistry 2004;12:3269–75.
[10] Gao H, Lei LD, Liu JQ, Kong Q, Chen XG, Hu ZD. The study on the interaction between human serum albumin and a new reagent with antitumour activity by spectrophotometric methods. Journal of Photochemistry and Photobiology A: Chemistry 2004;167:213–21.
[11] Sudlow G, Birkett DJ, Wade DN. The characterization of two specific drug binding sites on human serum albumin. Molecular Pharmaceutics 1975;11:824–32.
[12] Curry S, Mandelkow H, Brick P, Franks N. Crystal structure of human serum albumin complexed with fatty acid reveals an asymmetric distribution of binding sites. Nature Structural & Molecular Biology 1998;58:827–35.
[13] Sadler PJ, Tucker A, Viles JH. Involvement of a lysine residue in the N-terminal $Ni^{2+}$ and $Cu^{2+}$ binding site of serum albumins. European Journal of Biochemistry 1994;220:193–200.
[14] Bar-Or D, Lau E, Winkler JV. A novel assay for cobalt-albumin binding and its potential as a marker of myocardial ischemia: a preliminary report. Journal of Emergency Medicine 2000;19:311–5.
[15] Eftink MR, Ghiron CA. Fluorescence quenching of indole and model micelle systems. The Journal of Physical Chemistry 1976;80:486–93.
[16] Dong AC, Huang P, Caughey WS. Protein secondary structures in water from second-derivative amide I infrared spectra. Biochemistry 1990;29:3303–8.
[17] He WY, Li Y, Si HZ, Dong YM, Sheng FL, Yao XJ, et al. Molecular modeling and spectroscopic studies on the binding of guaiacol to human serum albumin. Journal of Photochemistry and Photobiology A: Chemistry 2006;182:158–67.
[18] Khan AM, Muzammil S, Musarrat J. Differential binding tetracyclines with serum albumin and induced structural alterations in drug-bound protein. International Journal of Biological Macromolecules 2002;30:243–9.
[19] Petitpas I, Bhattacharya AA, Twine S, East M, Curry S. Crystal structure analysis of warfarin binding to human serum albumin. Journal of Biological Chemistry 2001;276:22804–9.
[20] Morris G. SYBYL software, version 6.9. St. Louis: Tripos Associates Inc; 2002.

[21] Gong AQ, Zhu XS, Hu YY, Yu SH. Monitoring of environmental phenolic endocrine disrupting compounds in treatment effluents and river waters, Korea. Talanta 2007;73:668–73.
[22] Scatchard G. The attractions of protein for small molecules and ions. Annals of the New York Academy of Sciences 1949;51:660–73.
[23] Ross PD, Subramanian S. Thermodynamics of protein association reactions: forces contributing to stability. Biochemistry 1981;20:3096–102.
[24] Miller JN. Recent advances in molecular luminescence analysis. Proceedings of the Analytical Division of the Chemical Society 1979;16:203–8.
[25] Witold KS, Henry HM, Dennis C. De-termination of protein secondary structure by transform infrared spectroscopy: a critical assessment. Biochemistry 1993;32:389–94.
[26] Yang P, Gao F. Theory of bioinorganic chemistry. Beijing: Science Press; 2002.
[27] Forster T. In: Sinanoglu O, editor. Modern quantum chemistry, vol. 3. New York: Academic Press; 1996. p. 93.
[28] Cyril L, Earl JK, Sperry WM. Biochemists handbook. London: E & FN Epon Led. Press; 1961.
[29] Tang JH, Luan F, Chen XG. Binding analysis of glycyrrhetinic acid to human serum albumin: fluorescence spectroscopy, FTIR, and molecular modeling. Bioorganic & Medicinal Chemistry 2006;14:3210–7.
[30] Zhang GC, Wang YQ, Zhang HM, Tang SH, Tao WH. Human serum albumin interaction with paraquat studied using spectroscopic methods. Pesticide Biochemistry and Physiology 2007;87:23–9.